NJC

Accepted Manuscript

This is an *Accepted Manuscript*, which has been through the Royal Society of Chemistry peer review process and has been accepted for publication.

Accepted Manuscripts are published online shortly after acceptance, before technical editing, formatting and proof reading. Using this free service, authors can make their results available to the community, in citable form, before we publish the edited article. We will replace this *Accepted Manuscript* with the edited and formatted *Advance Article* as soon as it is available.

You can find more information about *Accepted Manuscripts* in the Information for Authors.

Please note that technical editing may introduce minor changes to the text and/or graphics, which may alter content. The journal's standard Terms & Conditions and the Ethical guidelines still apply. In no event shall the Royal Society of Chemistry be held responsible for any errors or omissions in this *Accepted Manuscript* or any consequences arising from the use of any information it contains.

ROYAL SOCIETY OF CHEMISTRY

www.rsc.org/njc

Tunable luminescence and energy transfer properties of a novel $Na_4Ca_4Si_6O_{18}:Ce^{3+}$, Mn^{2+} phosphor

Dongxu Wei [a, b,*], Ying Sun [c], Lianzhou Jiang [a, *], Shaoxin Hu [a], Dan Li [a]

[a] College of Food Science, Northeast Agricultural University, Harbin, 150030, Heilongjiang, China

[b] Heilongjiang Entry-Exit Inspection and Quarantine Bureau, Harbin, 150001, Heilongjiang, China

[c] College of Tourism and Culinary, Harbin University of Commerce, Harbin, 150001, Heilongjiang, China

∗ Corresponding author:E-mail address: jianglianzhou@hotmail.com(L. Z. Jiang)

Tel. / fax: +86-431-8233-7563

Abstract: A series of color-tunable $Na_4Ca_4Si_6O_{18}:Ce^{3+}$, Mn^{2+} phosphors were synthesized via high-temperature solid-state reaction. The effect of Ce^{3+} concentration on the emission intensity of $Na_4Ca_4Si_6O_{18}:Ce^{3+}$ is studied, and the energy transfer from Ce^{3+} to Mn^{2+} is observed. The emission spectra of the $Na_4Ca_4Si_6O_{18}:Ce^{3+}$, Mn^{2+} phosphors show a blue band at 430 nm of Ce^{3+} and a red band at 590 nm of Mn^{2+}, originated from the allowed 5d → 4f transition of the Ce^{3+} ion and the $^4T_{1g}(4G) \rightarrow {}^6A_{1g}(6S)$ transition of the Mn^{2+} ion, respectively. Non-radiative transitions between the Ce^{3+} and Mn^{2+} ions in the $Na_4Ca_4Si_6O_{18}$ host is demonstrated to be dipole-quadrupole interactions. Results indicate that the varied emitted color from blue to red can be achieved by tuning the relative ratio of the Ce^{3+} to Mn^{2+} ions based on the principle of energy transfer. We have demonstrated that $Na_4Ca_4Si_6O_{18}:Ce^{3+},Mn^{2+}$ phosphors can be a promising candidate for a color-tunable phosphor applied in a near-UV white LEDs.

1. Introduction

Phosphor materials are widely used in various application such as fluorescent lamps, cathode ray tubes, vacuum fluorescent display, plasma display, LED, polyhouses etc. [1,2] Different types of phosphors with blue, red, green, and sometimes with dual emission characteristics are required for technological applications. Many of the phosphors presently used are obtained by doping rare earth ions into host material. In particular, Ce^{3+}-activated phosphors were invented with remarkable properties for white LEDs applications, such as the commonly used down converting yellow emitting $Y_3Al_5O_{12}:Ce^{3+}$ phosphor and silicate garnet $Sr_3SiO_5:Ce^{3+}$ and $Ca_3Sc_2Si_3O_{12}:Ce^{3+}$ phosphors.[3-5] On the other hand, Ce^{3+} ion can also act as an excellent sensitizer, transferring a part of its energy to activator ion such as Mn^{2+}.[6-15] As we known, The Mn^{2+} ion has abroad emission band and usually gives an orange or red emission. Owing to the spin forbidden $^4T_1–^6A_1$ transition, the emission intensity of Mn^{2+}-doped phosphor is weak under UV excitation. Thus, the Mn^{2+} emission can be realized efficiently by energy transfer from Ce^{3+} to Mn^{2+}, which plays an important role in development of efficient phosphor materials. [16-26]

Recently, many efforts have been made to develop phosphors using energy transfer from Ce^{3+} to Mn^{2+}. Controlling the dopant concentrations in the hosts causes the emitting color to move from the blue/green to the orange/red region. For example, Li et al. reported a single-component color-tunable $CaSr_2Al_2O_6:Ce^{3+}$, Li^+, Mn^{2+} phosphors. By codoping the Ce^{3+} and Mn^{2+} ions into the host and utilizing the energy transfer, the color hues can be varied from blue to red.[27] Lu et al. incorporated Mn^{2+} into and

consequently generated an orange emission band peaking at 572 nm.[28] In this work, we have demonstrated a novel dual-tunable $Na_4Ca_4Si_6O_{18}$: Ce^{3+}, Mn^{2+} phosphor by energy transfer mechanism between the luminescence centers Ce^{2+} and Mn^{2+}. We have also proven that the varied emitted color from blue to red can be achieved by increasing the dopant contents of Mn^{2+}. The $Na_4Ca_4Si_6O_{18}$: Ce^{3+}, Mn^{2+} phosphor exhibits great potential for use in near UV-LED applications.

2. **Experimental**

All samples $Na_4Ca_{4-x-y}Si_6O_{18}$:xCe^{3+},yMn^{2+} (abbreviated as NCSO:xCe^{3+},yMn^{2+}; x, y are mol%)) were synthesized by a high-temperature solid-state reaction. The constituent oxides or carbonates Na_2CO_3 (A.R.), $CaCO_3$ (A.R.), SiO_2 (A.R.), CeO_2 (A.R.), and $MnCO_3$ (A.R.) were thoroughly mixed by grinding, and then sintered in a tubular furnace at 1150°C for 4 h in CO reducing atmosphere. Powder X-ray diffraction (XRD) data was collected using Cu Kα radiation (λ = 1.54056 Å) on a Bruker D8 Advance diffractometer equipped with a linear position-sensitive detector (PSD-50m, M. Braun), operating at 40 kV and 40 mA with a step size of 0.02° (2θ). Crystal structure refinement employed the Rietveld method as implemented in the General Structure Analysis System (GSAS) program.[29] The measurements of photoluminescence (PL) and photoluminescence excitation (PLE) spectra were performed by using a Hitachi F4500 spectrometer equipped with a 150 W xenon lamp under a working voltage of 700 V. In fluorescence lifetime measurements, the third harmonic (355 nm) of an Nd-doped yttrium aluminum garnet pulsed laser (Spectra- Physics, GCR 130) was used as an excitation source, and the signals were detected with a Tektronix digital oscilloscope

(TDS 3052).

3. Results and Discussion

The initial model compound $Na_4Ca_4Si_6O_{18}$ belongs to a typical hexagonal structure with P 3_121 symmetry. In order to further study the crystal structure of the as-prepared phosphors, the Rietveld structural refinement for the selected composition of NCSO:0.04Ce^{3+} is performed. Figure 1 shows the experimental, calculated and their difference results of the XRD refinement of NCSO:0.04Ce^{3+} sample. The initial structural model was constructed with crystallographic data previously reported for $Na_4Ca_4Si_6O_{18}$ (JCPDS 79-1089). The crystallographic data, details on the data collection and refinement parameter are listed in Tables S1 in the Supporting Information. All of the observed XRD peaks are obtained with goodness of fit parameters R_{wp} = 11.01%, R_p=7.54% and χ^2 =6.35. NCSO crystallizes as a hexagonal structure with a space group of P $3_121$and lattice constants of a=b=10.4728 Å, c=13.1537 Å. It is also found from the refinement result that Ca^{2+} ions have two different coordination numbers (CNs) as shown in Figure 1 inset. Ca(1) are coordinated with six oxygen and Ca(2) are seven oxygen atoms, respectively. In this study, in the view of effective ionic radii, Si^{4+} (0.26 Å), Ca^{2+}(1.00 Å), Ce^{3+} (1.01 Å) and Mn^{2+} (0.66 Å), it is concluded that Ce^{3+} and Mn^{2+} are expected to occupying the Ca^{2+} sites preferably because the four-coordinated Si^{4+} sites are too small for these ions to replace them. Furthermore, Figure S1 depicts the XRD patterns of the NCSO: 0.04Ce^{3+}, yMn^{2+}. All of the diffraction peaks are indexed to the standard data of $Na_4Ca_4Si_6O_{18}$ (JCPDS 79-1089) and no diffraction peaks from the raw materials are detected. It can be seen

that the as-prepared samples shifted to higher angles with increasing Mn content (y value) owing to the radius difference between Mn^{2+} and Ca^{2+}. This result futher suggests that the Ca^{2+} ions are substituted by the smaller Mn^{2+} ions.

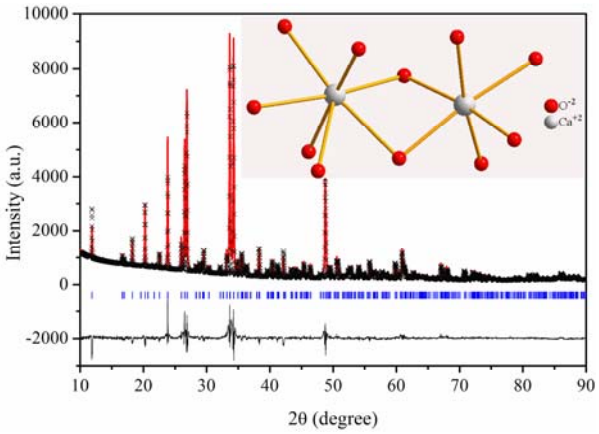

Fig. 1 Rietveld analysis patterns for X-ray powder diffraction data of NCSO:0.04Ce^{3+}. The crosses marks represent the experimental intensities, and the red solid line is the calculated one. A difference (obsd - calcd) plot is shown beneath. Tick marks above the difference data indicate the reflection positions.

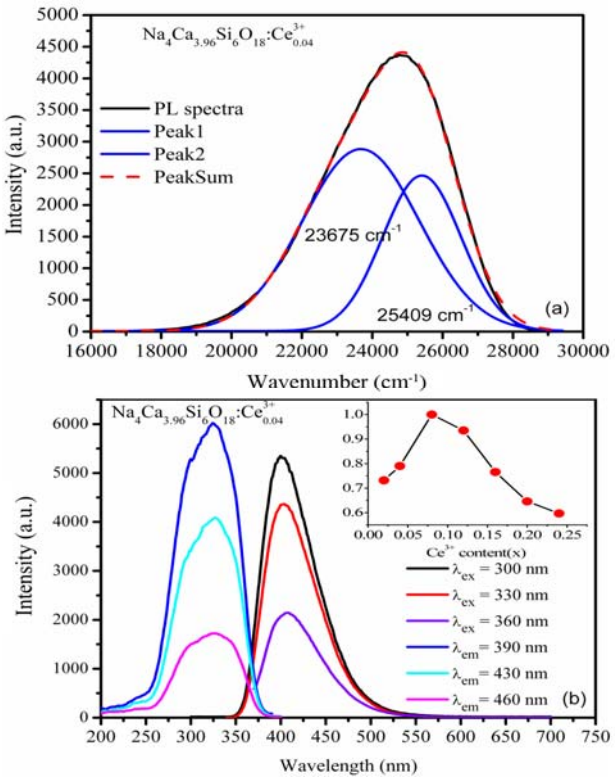

Fig. 2 Gaussian fitting of the emission band (a) and PL and PLE spectra (b) of the NCSO:0.04Ce^{3+} phosphor. Inset: the PL intensity as a function of x upon 330 nm excitation.

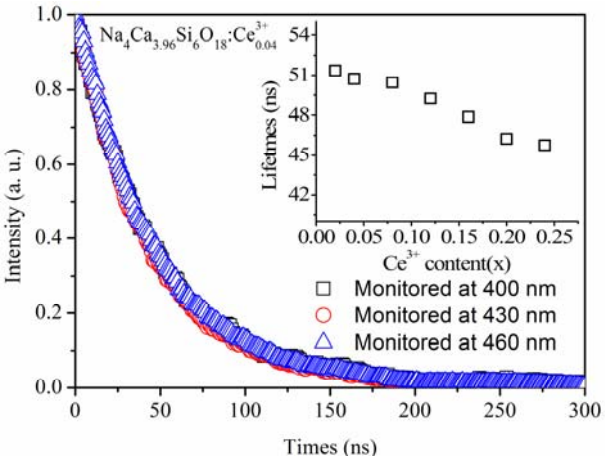

Fig.3 Fluorescence lifetimes of NCSO:0.04Ce^{3+} phosphor with monitored at different wavelength. The inset is the dependence of the fluorescence lifetimes on Ce^{3+} concentration.

Figure 2 (a) and (b) depicts the PL and PLE spectra of the NCSO:0.04Ce^{3+} phosphor. The sample shows a broad intense excitation band from 250 to 400 nm due to the $4f^7 \rightarrow 4f^6 5d^1$ transition of the Ce^{3+} ions. At the excitation of 330 nm, the PL spectrum shows an intense blue emission band attributed to the $4f^6 5d^1 \rightarrow 4f^7$ transition of the Ce^{3+} ion. The asymmetric emission band under the excitation of 330 nm can be fitted to two Gaussian profiles centered at 422 nm (23675 cm^{-1}) and 393 nm (25409 cm^{-1}), which is also similar to the theoretical value of 2000cm^{-1} for $^2F_{7/2}$ and $^2F_{5/2}$ ground states of Ce^{3+}. It is obvious that there are little changes in the blue emission except the emission intensity when varying the excitation wavelength from 330 to 360 nm. This means that Ce^{3+} ions only occupy the Ca(1) or Ca(2) site in the NCSO lattice. To investigate the effect of doping concentration on luminescence properites, a series of NCSO:xCe^{3+} with

varying Ce^{3+} contents (x=0.02, 0.04, 0.08, 0.12, 0.16, 0.20 and 0.24) are synthesized. Figure 2(b) inset shows the concentration dependence of PL intensity of NCSO:xCe^{3+}. The PL intensity increases with increasing Ce^{3+} concentration and reaches a maximum when x=0.08. Beyond this value, the PL intensity is found to decrease due to concentration quenching. Decay curves of NCSO:0.04Ce^{3+} and the dependence of the fluorescence lifetimes on Ce^{3+} concentration are depicted in Figure 3. When monitored at different wavelength, the decay time of Ce^{3+} do not changes, further supporting that Ce^{3+} ions substitute only one site (Ca(1) or Ca(2)) in NCSO. The decay lifetime for the Ce^{3+} ions is found to slightly decrease with the increase in Ce^{3+} contents, which is due to the nonradiative energy transfer between Ce^{3+} ions.

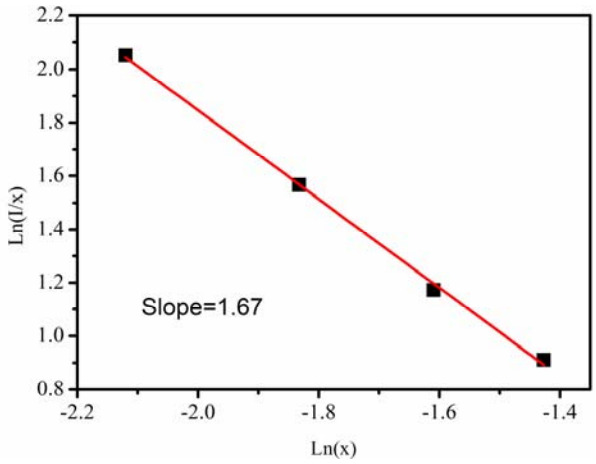

Fig. 4 The fitting curve of ln(I/x) versus ln(x) in NCSO:xCe^{3+} phosphors.

If the energy transfer occurs between the same sorts of activators, then the intensity of the multipolar interaction can be determined from the change of the emission intensity from the emitting level which has a multipolar interaction. The emission intensity (I) per activator ion follows the equation:[30]

$$I / x = k\left[1+\beta\left(x\right)^{\theta/3}\right]^{-1} \qquad (1)$$

Where x is the activator concentration, I/x is the emission intensity per activator

concentration, k and β are constants for a given host in the same excitation condition, θ = 6, 8 and 10 represent the dipole–dipole, dipole–quadrupole, and quadrupole–quadrupole interactions, respectively. By modifying the Eq. 1, log(I/x) acts a liner function of log(x) with a slop of (-θ/3). From Figure 4, the θ/3 is determined to be 1.67 and accordingly, θ is calculated to be 5.01 which is close to 6. The result indicates that the concentration quenching mechanism of the Ce^{2+} emission in NCSO host is dominated by the dipole-dipole interaction.

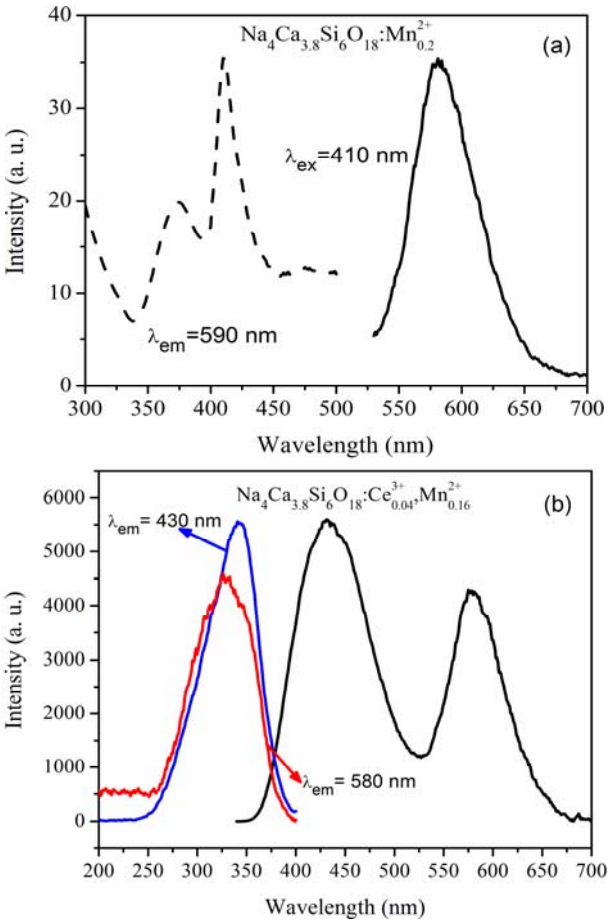

Fig. 5 PLE and PL spectra of (a) NCSO: 0.1Mn^{2+} and (b) NCSO: 0.04Ce^{3+}, 0.16Mn^{2+} phosphors.

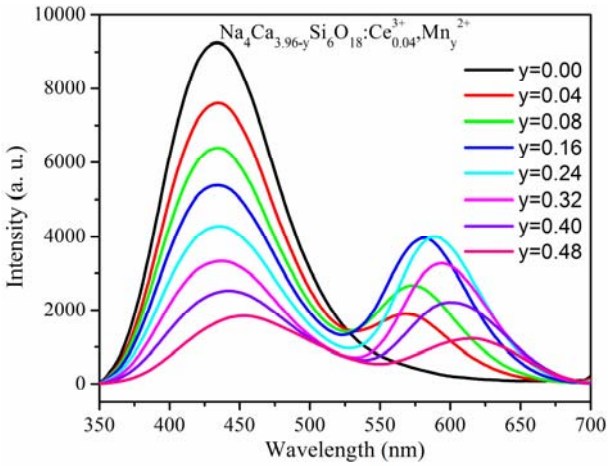

Fig. 6 PL spectra of NCSO: $0.04Ce^{3+}$, yMn^{2+} with various Mn^{2+} contents.

The excitation and emission spectra of the Mn^{2+} singly doped phosphors is shown in Figure 5(a). The d-d transitions of Mn^{2+} are forbidden in view of spin and parity, so their excitation transitions are difficult to pump and emission intensity is very weak. NCSO: $0.1Mn^{2+}$ phosphor presents a band broad emission band centered at 590 nm, which corresponds to the $^4T_1(^4G) \rightarrow {}^6A^1(^6S)$ transition of Mn^{2+}. Its excitation spectrum consists of several bands centered at 359 and 410 nm, which are assigned to the transitions from $^6A_1(6S)$ to $^4T_2(4D)$ and $^4T_2(^4G)$ levels of Mn^{2+}, respectively. The intensity of the Mn^{2+} emission is weaker than that of the Ce^{3+} emission in the NCSO host, which is due to the forbidden d-d transition of Mn^{2+}. We have observed a significant spectral overlap between the Ce^{3+} PL and Mn^{2+} PLE spectra, indicating the possibility of energy transfer from Ce^{3+} to Mn^{2+} in NCSO. Figure 5(b) illustrates the PLE and PL spectra of NCSO: $0.04Ce^{3+}$, $0.16Mn^{2+}$. It is found that the PLE spectrum of the Mn^{2+} is similar to that of Ce^{3+}, demonstrating the existence of energy transfer from Ce^{3+} to Mn^{2+} in NCSO systems. Figure 6 gives the emission spectra of Ce^{3+}, Mn^{2+} co-doped NCSO as a function of Mn^{2+} concentrations (y=0, 0.04, 0.08, 0.16, 0.24, 0.32,

0.40 and 0.48). The emission intensity of Ce^{3+} gradually decreases. Meanwhile, the emission intensity of the Mn^{2+} ions increases initially and reaches a maximum at y = 0.24, beyond which it decreases ascribed to the Mn^{2+} – Mn^{2+} internal concentration quenching. Furthermore, the emission peaks of the Ce^{3+} and Mn^{2+} ions show a red-shift as the Mn^{2+}content increases. Since a smaller Mn^{2+} ion substitution on Ca^{2+} sites causes a shrinking of bond lengths as confirmed by the XRD pattern, which finally results in this phenomenon.

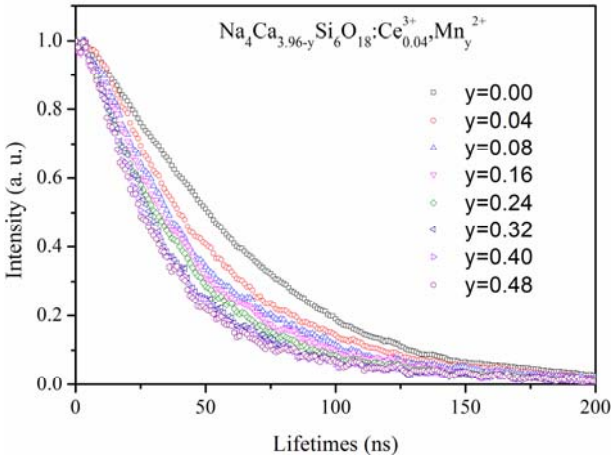

Fig.7 PL decay curves of the Ce^{3+} emission in NCSO: $0.04Ce^{3+}$, yMn^{2+} under excitation at 355 nm, monitored at 430 nm.

In order to investigate the luminescence dynamics of the samples, we measured the PL decay curves and then calculated the lifetime as well as energy transfer efficiencies, as shown in Figure 7 and 8. The fluorescence of Ce^{3+} decays faster and tends to be a nonexponential function with increasing the Mn^{2+} concentration, as shown in Figure 7. The decay process of these samples is characterized by an average lifetime τ, which can be calculated using Eq. 1 as follows

$$\tau_{avg} = \int_0^\infty I(t)tdt \Big/ \int_0^\infty I(t)dt \qquad (2)$$

where the $I(t)$ represents the luminescence intensity at time t. From Eq. 2, the lifetime of

Ce^{3+} decreases with increasing Mn^{2+} concentration, which are 64.33, 55.96, 50.53, 47.12, 43.91, 41.16 , 39.91 and 39.75 ns, respectively. The decay lifetime for the Ce^{3+} ions is found to reduce with increasing Mn^{2+} doping content, strongly demonstrating the energy transfer from the Ce^{3+} to Mn^{2+} ions.

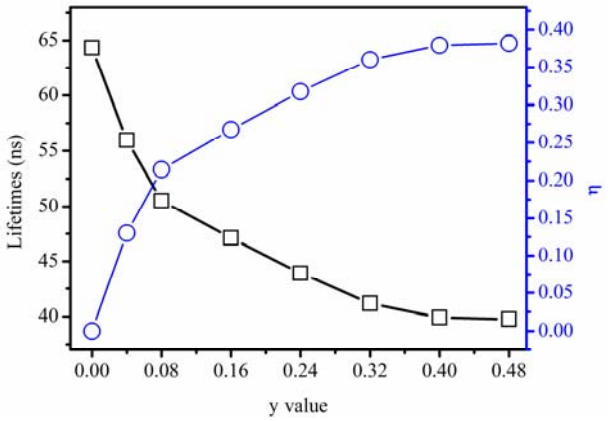

Fig.8 Lifetimes and the energy transfer efficiency of NCSO: $0.04Ce^{3+}$,yMn^{2+} as a function of Mn^{2+} concentration.

The energy transfer efficiency (η) from the Ce^{3+} to Mn^{2+} ions in the NCSO:Ce^{3+},yMn^{2+} phosphors can be calculated by using the following formula

$$\eta = 1 - \tau / \tau_0, \qquad (3)$$

where τ_0 is the lifetime of the Ce^{3+} ions in the absence of the Mn^{2+} ions and τ is the lifetime of the Ce^{3+} ions in the presence of the Mn^{2+} ions. The η is calculated as a function of Mn^{2+} concentration y and represented in the Figure 8. It can be seen that the values η gradually increases and reaches 38% for Mn^{2+} concentrations at y = 0.48. This value η is higher than that of $CaSr_2Al2O_6$:Ce^{3+}, Li^+, Mn^{2+} (27%) but lower than that of $Ca_3Sc_2Si_3O_{12}$:Ce^{3+}, Li^+, Mn^{2+} (45%).[7,27]

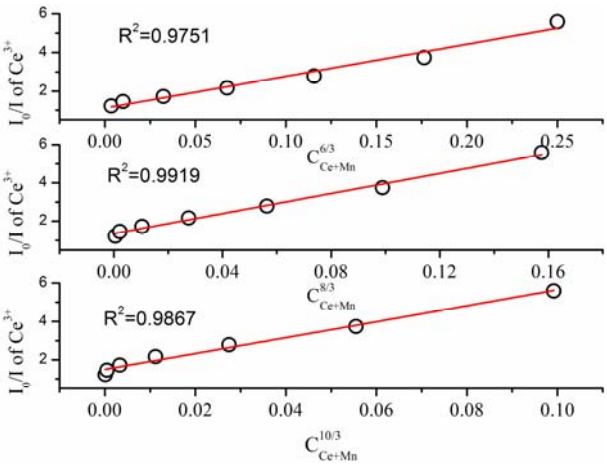

Fig. 9 Experimental data plots of I/I_0 versus $C^{n/3}$. The red lines indicate the fitting behaviors.

In many cases, concentration quenching is due to energy transfer from one activator to another until an energy sink in the lattice is reached. The critical distance R_C for energy transfer from the Ce^{3+} to Mn^{2+} ions can be calculated using the concentration quenching method. According to Blasse, [31] the critical distance R_C can be expressed by

$$R_C \approx 2\left[\frac{3V}{4\pi X_c N}\right]^{1/3} \quad (4)$$

where V is the volume of the unit cell, N is the number of available sites for the dopant in the unit cell, X is the total concentration of Ce^{3+} and Mn^{2+},. For the $Na_4Ca_4Si_6O_{18}$ host, N = 12 and V=1257.84 $Å^3$. The critical concentration X_C, at which the luminescence intensity of Ce^{3+} is half of that in the absence of Mn^{2+} is 0.24. Therefore, the critical distance (R_C) of energy transfer was calculated to be about 9.41 Å.

According to Dexter's energy transfer expressions of multipolar interaction and Reisfeld's approximation, the following relation can be given as [32]

$$\frac{I_0}{I} \propto C^{n/3} \quad (5)$$

where C is the sum of the content of Ce^{3+} and Mn^{2+}. The plots of (I_0/I) versus $C^{n/3}$ with n= 6, 8, and 10 correspond to dipole-dipole, dipole-quadrupole and quadrupole-quadrupole interactions. Figure 9 illustrates the relationships between (I_0/I) versus $C^{n/3}$, and a liner relation is observed when n = 8. This clearly indicates that the energy transfer mechanism from the Ce^{3+} to Mn^{2+} ions is a dipole-quadrupole reaction. Considering dipole−quadrupole interaction, the critical distance from the sensitizer to the acceptor can also be calculated by the spectral overlap method, as expressed as follows:[30,32]

$$R_C^8 = 3.024 \times 10^{12} \lambda_S^2 f_q \int \frac{F_S(E) F_A(E) dE}{E^4} \quad (6)$$

where f_q ($=10^{-10}$) is the oscillator strength of the involved absorption transition of the acceptor (Mn^{2+}), λ_S (in Å) is the wavelength position of the sensitizer's emission, E is the energy involved in the transfer (in eV), and $\int F_S(E) F_A(E) / E^4 dE$ represents the spectral overlap between the normalized shapes of the Ce^{3+} emission $F_S(E)$ and the Mn^{2+} excitation $F_A(E)$, and in our case, it is calculated to be about 0.01256 eV^{-4}. Using Eq. 6, the critical distance R_C was estimated to be 9.59 Å. This result is in good agreement with that obtained using the concentration quenching method, which further reveals that the mechanism of energy transfer from the Ce^{3+} to Mn^{2+} ions is mainly due to a dipole-quadrupole interaction.

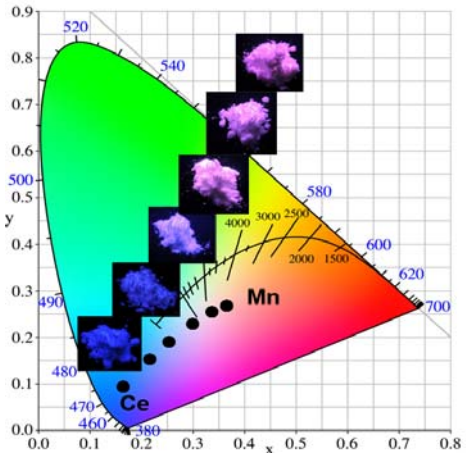

Fig. 10 CIE chromaticity diagram of NCSO: $0.04Ce^{3+}$, yMn^{2+} phosphors under 330 nm excitation and corresponding selected phosphors images excited at 365 nm in the ultraviolet (UV) box.

The CIE chromaticity coordinates of the NCSO:$0.04Ce^{3+}$,yMn^{2+} with different dopant contents are measured and presented in Figure 10. With increasing Mn^{2+} content, the (x,y) coordinates of NCSO: $0.04Ce^{3+}$, yMn^{2+} phosphors vary systematically from (0.16, 0.10), (0.21, 0.17), (0.24, 0.21), (0.30, 0.25) to (0.33, 0.25), and correspondingly, the color tone of the phosphors shifts gradually from blue to red with increasing the content of Mn^{2+}. As the contents of Mn^{2+} further increase to 0.32 and 0.48, the value CIE chromaticity of phosphor do not change remarkably, this may be due to the effect of concentration quenching from Mn^{2+}.

4. **Conclusion**

In summary, a new blue and red dual $Na_4Ca_4Si_6O_{18}$: Ce^{3+}, Mn^{2+} phosphors are synthesized. The effect of Ce^{3+} concentration on the emission intensity and energy transfer from sensitizer Ce^{3+} to activator Mn^{2+} in $Na_4Ca_4Si_6O_{18}$ host have been studied. The energy transfer from Ce^{3+} to Mn^{2+} in $Na_4Ca_4Si_6O_{18}$ phosphors have been demonstrated to be a resonant type via a dipole−quadrupole mechanism，and the critical

distance (R_C) calculated by quenching concentration method and spectral overlap method are 9.41 Å and 9.59 Å, respectively. The emission color of the obtained phosphors can be easily modulated from blue to red by simply adjusting the amount of Mn^{2+} ions due to the different emission compositions of the Ce^{3+} and Mn^{2+} ions. These results indicated that $Na_4Ca_4Si_6O_{18}:Ce^{3+}$, Mn^{2+} may serve as a potential color-tunable near UV phosphor for white-light LED devices.

Acknowledgments

The authors would like to thank the Natural Science Foundation of China (Project No. 31071493), the Heilongjiang Science and Technology Agency (research grant number: GA09B401-6), the Ministry of Agriculture of Modern Technology System Projects the Soybean Industry (research grant number: nycytx-004), the National Research Center of Soybean Engineering and Technology, and the Northeast Agricultural University for funding this study.

References:

1 S. Nakamura and G. Fasol, The Blue Laser Diod Springer Berlin 1997, 216.

2 E.F. Schubert and J. K. Kim, *Science.*, 2005, **308**, 1274.

3 S. Lee and S. Y. Seo, J. *Electrochem. Soc.,* 2002, **149**, J85.

4 H. S. Jang and D. Y. Jeon, *Appl. Phys.Lett.*, 2007, **90**, 0419061.

5 Y. Shimomura, T. Honma, M. Shigeiwa, T. Akai, K. Okamoto and N. Kijima, *J. Electrochem. Soc.*, 2007, **154**, J35.

6 X. Zhang and M. Gong, *Mater. Lett.*, 2011, **65**, 1756.

7 Y. Liu, X. Zhang, Z. Hao, Y. Luo, X. Wang and J. Zhang, *J. Mater. Chem.*, 2011, **21**, 16379.

8 G. Zhu, Y. Wang, Z. Ci, B. Liu, Y. Shi and S. Xin*, J. Electrochem. Soc.,* 2011, **158 (8)**, J236.

9 G. G. Li, D. L. Geng, M. M Shang, C. Peng, Z. Y. Chen and J. Lin, *J. Mater. Chem.*, 2011, **21**, 13334.

10 Y. F. Liu, X. Zhang, Z. D. Hao, Y. S. Luo, X. J. Wang and J. H. Zhang, *Chem. Commun.,* 2011, **47**, 10677.

11 G. G. Li, D. L. Geng, M. M Shang, Y. Zhang, C. Peng, Z. Y. Chen, J. Lin, *J. Phys. Chem. C.*, 2011, **115**, 21882.

12 Y. C. Jia, Y. J. Huang, N. Guo, H. Qiao, Y. H. Zheng, W. Z. Lv, Q. Zhao and H. P. You, *J. Mater. Chem.,* 2012, **22**, 15146.

13 W. Lu, N. Guo, Y. C. Jia, Q. Zhao, W. Z. Lv, M. M. Jiao, B. Q. Shao and H. P. You, *Inorg. Chem.*, 2013, **52**, 3007.

14 M. M. Shang, D. L. Geng, Y. Zhang, G. G. Li, D. M. Yang, X. J. Kang and J. Lin, *J. Mater. Chem.,* 2012, **22**, 19094.

15 G. G. Li, Y. Zhang, D. L. Geng, M. M. Shang, C. Peng, Z. Y. Cheng and J. Lin, *ACS Appl. Mater. Interfaces.*, 2012, **4 (1)**, 296.

16 W. Lu, Y. C. Jia, W. Z. Lv, Q. Zhao and H. P. You, *New J. Chem.*, 2013, **37**, 3701.

17 Y. Li, Y. Shi, G. Zhu, Q. Wu, H. Li, X. Wang, Q. Wang and Y. Wang, *Inorg. Chem.*, 2014, **53**, 7668.

18 J. Zhang, Y. He, Z. Qiu, W.Zhang, W. Zhou, L. Yu and S. Lian, *Dalton Trans.*,

2014, **43**, 18134.

19 J. Qiao, J. Zhang, X. Zhang, Z. Hao, Y. Liu and G. Pan, *Opt. Lett.*, 2014, **39**, 2691.

20 M. Jiao, Y. Jia, W. Lu, W. Lv, Q. Zhao, B. Shao and H. You, *Dalton Trans.*, 2014, **43**, 3202.

21 W. Lu, Y. Jia, Q. Zhao, W. Lv and H. You, *Chem. Commun.*, 2014, **50**, 2635.

22 V. C. Teixeira, P.J. R. Montes and M. E. G. Valerio, *Opt. Mater.*, 2014, **36**, 1580.

23 X. Zhang, M. Gong, *Dalton Trans.*, 2014, **43**, 2465.

24 Q. Wang, Z. Ci, Y. Wang, G. Zhu, Y. Wen and Y. Shi, *Mater. Res. Bull.*, 2013, **48**, 1065.

25 G. G. Li and J. Lin, *Chem. Soc. Rev.*, 2014, **43**, 7099.

26 X. Dong, J. Zhang, X. Zhang, Z. Hao and Y. Luo, *J. Lumin.*, 2014, **148**, 60.

27 Y. Li, Y. Shi, G. Zhu, Q.Wu, H. Li, X. Wang, Q. Wang and Y. Wang, *Inorg. Chem.*, 2014, **53**, 7668.

28 W. Lu, W. Z. Lv, Q. Zhao, M. M. Jiao, B. Q. Shao and H. P. You, *J. Mater. Chem.*, C, 2015, **3**, 2334.

29 A. C. Larson and R. B. Von Dreele, Los Alamos Natl. Lab, LAUR; 1994, 86-748.

30 D. L. Dexter, *J. Chem. Phys.*, 1953, **21**, 836.

31 Blasse, G. *Philips Res. Rep.,* 1969, **24**, 131.

32 D. L. Dexter and J. H. Schulman, *J. Chem. Phys.*, 1954, **22**, 1063.